



HAL
open science

Gene expression profiling identifies emerging oncogenic pathways operating in extranodal NK/T-cell lymphoma, nasal type.

Yenlin Huang, Aurélien de Reyniès, Laurence de Leval, Bouchra Ghazi, Nadine Martin-Garcia, Marion Travert, Jacques Bosq, Josette Brière, Barbara Petit, Emilie Thomas, et al.

► To cite this version:

Yenlin Huang, Aurélien de Reyniès, Laurence de Leval, Bouchra Ghazi, Nadine Martin-Garcia, et al.. Gene expression profiling identifies emerging oncogenic pathways operating in extranodal NK/T-cell lymphoma, nasal type.. *Blood*, 2010, 115 (6), pp.1226-37. 10.1182/blood-2009-05-221275 . inserm-00462629

HAL Id: inserm-00462629

<https://inserm.hal.science/inserm-00462629v1>

Submitted on 10 Mar 2010

HAL is a multi-disciplinary open access archive for the deposit and dissemination of scientific research documents, whether they are published or not. The documents may come from teaching and research institutions in France or abroad, or from public or private research centers.

L'archive ouverte pluridisciplinaire **HAL**, est destinée au dépôt et à la diffusion de documents scientifiques de niveau recherche, publiés ou non, émanant des établissements d'enseignement et de recherche français ou étrangers, des laboratoires publics ou privés.

Gene expression profiling identifies emerging oncogenic pathways operating in extranodal NK/T-cell lymphoma, nasal-type

Yenlin Huang,^{1, 2, 3*} Aurélien de Reyniès,^{4*} Laurence de Leval,⁵ Bouchra Ghazi,⁶ Nadine Martin-Garcia,^{1, 2, 3} Marion Travert,^{1,2,3} Jacques Bosq,⁷ Josette Brière,⁸ Barbara Petit,⁹ Emilie Thomas,⁴ Paul Coppo,¹⁰ Teresa Marafioti,¹¹ Jean-François Emile,¹² Marie-Hélène Delfau-Larue,^{1, 2, 13} Christian Schmitt,⁶ and Philippe Gaulard^{1, 2, 3}

(1) INSERM U955, Créteil, France; (2) Université Paris 12, Faculté de Médecine, Créteil, France; (3) Département de Pathologie, AP-HP, Groupe Henri-Mondor Albert-Chenevier, Créteil, France (4) Ligue Nationale Contre le Cancer, Paris, France; (5) Pathology Department, CHU Sart Tilman, University of Liège, Liège, Belgium; (6) INSERM U976, Hôpital Saint-Louis, Paris, France; (7) Department of Medical Biology and Pathology, Institut Gustave Roussy, Villejuif, France; (8) INSERM U728 et Service de Pathologie, Hôpital Saint-Louis, Paris, France; (9) Département de Pathologie, CHU Dupuytren, Limoges, France; (10) Service d'Hématologie et de Thérapie Cellulaire, Hôpital Saint-Antoine and Université Pierre et Marie Curie, Paris, France; (11) The Nuffield Department of Clinical Laboratory Sciences, John Radcliffe Hospital, Oxford, United Kingdom, (12) Service de pathologie, Hôpital Ambroise Paré, AP-HP et EA4340, Université de Versailles, Saint-Quentin-en-Yvelines, France; (13) Laboratoire d'Immunologie Biologique, AP-HP, Groupe Henri-Mondor Albert-Chenevier, Créteil, France.

*Y.H. and A.d.R. contributed equally to this work

Presented in part at the XIVth Meeting of the European Association for Hematopathology / Society for Hematopathology, Bordeaux, France, September 22, 2008.

RUNNING TITLE: Molecular Signature of Nasal NK/T-cell Lymphomas

[WORD COUNTS FOR TEXT: 4944](#)

WORD COUNTS FOR ABSTRACT: 200

[REFERENCE COUNT: 50](#)

SCIENTIFIC CATEGORY: lymphoid neoplasia

ABSTRACT

Biopsies and cell lines of NK/T-cell lymphoma, nasal-type (NKTCL) were subject to combined gene expression profiling and array-based comparative genomic hybridization analyses. Compared to PTCL, NOS, NKTCL had higher transcript levels for NK-cell markers and cytotoxic molecules, especially granzyme H, a novel sensitive biomarker of NKTCL. Compared to normal NK cells, tumors were closer to activated than resting cells and overexpressed several genes related to vascular biology, EBV-induced genes and *PDGFRA*. Notably, *PDGFR α* and its phosphorylated form were confirmed at the protein level, and *in vitro* the MEC04 NKTCL-cell line was sensitive to imatinib. Deregulation of the AKT, JAK-STAT and NF- κ B pathways suggested by bioinformatical analysis, was corroborated by nuclear expression of phosphorylated AKT, STAT3 and RelA in NKTCL, and several deregulated genes in these pathways mapped to regions of recurrent copy number aberrations (*AKT3* (1q44), *IL6R* (1q21.3), *CCL2* (17q12), *TNFRSF21* (6p12.3)). Several features of NKTCL uncovered by this analysis (overexpression of VEGFA and its receptor KDR by the tumor cells, overexpression of *MET-HGF*) suggest perturbation of angiogenic pathways. Integrative analysis also evidenced deregulation of the tumor suppressor *HACE1* in the frequently deleted 6q21 region. This study highlights emerging oncogenic pathways in NKTCL and identifies novel diagnostic and therapeutic targets.

INTRODUCTION

Several NK/T-cell lymphoma entities have a predilection for extranodal locations. One of the most common of these overall rare lymphoma entities is NK/T cell lymphoma, nasal type (NKTCL). The disease, most prevalent in Asian, Central and South American populations, most commonly arises in the nasal cavity or adjacent structures, but can also occur in other extranodal sites.¹ This lymphoma exhibits an angiocentric and angiodestructive growth pattern characteristically associated with necrosis and ulceration. The tumor cells typically express CD2, cytoplasmic CD3 (CD3ε chain) and CD56, are negative for CD5, CD4 and CD8 and have a cytotoxic immunophenotype with expression of perforin, granzyme B (gzm B), and T cell-restricted intracellular antigen (TiA1). Most cases derive from NK cells and lack T-cell receptor (TCR) gene rearrangement while a small proportion of cases have the phenotype and genotype of cytotoxic $\gamma\delta$ or $\alpha\beta$ T cells. Accordingly, the expression of killer immunoglobulin-like receptors (KIRs) has been documented in these tumors.²

In virtually all cases, most neoplastic cells harbor clonal episomal Epstein-Barr virus (EBV), suggesting the implication of the virus in tumor pathogenesis. The genetic alterations of NKTCL reported in a few studies include gain on chromosome 2q, losses of chromosomes 6q and 1p, and occasional presence of isochromosome 7q.³⁻⁶

Even with intensive therapies combining multi-agent chemotherapy and involved field radiotherapy, the prognosis of NKTCL remains poor with 5-year overall survival ranging from 42% to 64% in four recent studies,⁷⁻¹⁰ and novel alternative approaches are needed. Several factors have been incriminated to account for aggressiveness or poor outcome, including Fas and p53 mutations,^{11,12} expression of the multidrug resistance (MDR) 1 gene product P-glycoprotein,¹³ absence of CD94 transcript¹⁴ and gzm B inhibitor PI9.⁹ However, the mechanisms involved in resistance to therapy remain poorly understood.

Genome-wide profiling studies of NKTCL are scarce,^{3,15} likely reflecting not only the rarity of the disease, but also quantitative and qualitative restrictions imposed by small and often necrotic diagnostic samples. In one recent study, Iqbal et al. focused on in-depth genomic and transcriptomic analysis of specific chromosomal regions, which led them to identify candidate suppressor genes mapping to 6q.⁵ In the current study, we analyzed a series of NKTCL samples in relation to normal cells and peripheral T-cell lymphoma, not otherwise specified (PTCL, NOS), with the aims to (1) characterize the molecular signature of this lymphoma entity, (2) explore some signaling pathways implicated in its pathogenesis, and (3) search for novel markers potentially useful for diagnosis and/or targetable by therapeutic agents.

PATIENTS, MATERIALS AND METHODS

Patient characteristics and tumor samples

Nine newly diagnosed, previously untreated NKTCL patients with high quality RNA and/or DNA extracted from frozen tumor biopsies containing more than 60% tumor cells were selected for this study. Their main clinical, phenotypic and molecular characteristics are summarized in Table 1. Seven tumors originated in the nasopharyngeal area, one in the skin, and one in the hypophysis. All cases were reviewed by three hematopathologists (L.d.L, Y.H. and P.G.) and diagnosed according to the WHO criteria.¹ All cases had a CD3+ (cytoplasmic), CD2+, CD7+, CD5-, CD4-, CD8-, TiA1+, gzm B+ phenotype. Eight cases were positive for EBV by in situ hybridization with EBERs probes. A high load of EBV DNA was demonstrated by PCR in the remaining case. Specimens were also investigated for TCR γ chain gene rearrangement using a GC-clamp multiplex polymerase chain reaction (PCR)- γ -DGGE procedure. Seven cases without clonal T-cell population were regarded as of NK-cell origin, and a cytotoxic T-cell derivation was established in two cases with a clonal TCR gene

rearrangement. For immunohistochemical validation, formalin-fixed, paraffin-embedded tumor samples from 16 NKTCL, including seven of the cases described above, and 17 PTCL, NOS were selected.

The present study was approved by the institutional review board “Comité de Protection des Personnes Ile de France IX”, Créteil, France.

Cell lines and normal NK cells

Two NKTCL cell lines, SNK6 and SNT8 (Table 1),¹⁶ and two samples of normal CD56+ NK cells purified from peripheral blood including resting and IL-2-activated NK cells, were also subjected to gene expression profiling. The MEC04 NKTCL cell line was also used for *in vitro* proliferation assay and immunohistochemical validation.¹⁷ U937, a myelomonocytic cell line (ATCC LGC Standards, Molsheim, France), was used as control for *in vitro* assay. Cell lines were cultured in RPMI 1640 supplemented with 2 mM L-glutamine and 10% heat-inactivated fetal bovine serum (Invitrogen, Carlsbad, CA) in the presence of 100 U/ml recombinant human IL-2, except for U937 cell line. Centrifuged pellets of SNK6 and MEC04 cells were fixed in ethanol to construct paraffin-embedded blocks.

RNA and DNA extraction

Total RNA was extracted with TRIZOL reagent (Invitrogen, Carlsbad, CA), according to the manufacturer's instructions, and DNA was extracted with phenol-chloroform using standard procedures. The integrity of the extracts was verified on an Agilent 2100 Bioanalyser (Agilent Technologies, Palo Alto, CA, USA).

Microarray procedures

Microarray analyses were performed using 3 µg total RNA as starting material and 10 µg cRNA per hybridization (GeneChip Fluidics Station 400; Affymetrix, Santa Clara, CA). The total RNAs were amplified and labeled following the one-cycle target labeling protocol (<http://www.affymetrix.com>). The labeled cRNAs were hybridized to HG-U133 plus 2.0 Affymetrix GeneChip arrays (Affymetrix, Santa Clara, CA). The chips were scanned with an Affymetrix GeneChip Scanner 3000 and subsequent images analyzed using GCOS 1.4 (Affymetrix).

Gene expression analyses

The gene expression analysis encompassed HG-U133 plus 2.0 Affymetrix array data from seven NKTCL biopsies, two NKTCL cell lines (Table 1), 16 PTCL, NOS recently reported by our group under accession number E-TABM-702,¹⁸ six normal NK cells samples (including four previously published from GSE8059),¹⁹ [eighteen recently published normal B cell samples \(eight from GSE15271 and 10 from GSE12195\),^{20,21}](#) and 15 activated B-cell-like diffuse large B-cell lymphoma (ABC-DLBCL) samples from GSE12195.²¹ Two NK cell samples without stimulation of IL-2 (one each from ours and from GSE8059) represented the “resting NK cell” group, while the two NK cell samples stimulated by IL-2 for 24 hours (one from our sample, the other from GSE8059) were regarded as the “activated NK cell” group. Affymetrix raw data of the samples were normalized in batch using Robust Multichip Average (RMA) method along with 58 other samples unrelated to this study. The clustering analysis of the 25 tumor samples was performed as already described.²² To identify genes differentially expressed between two groups of samples we used Welch’s T-tests. To control for multiple testing, we measured the local false discovery rate using kerfdr R package, [an alternative approach to the more commonly used Bonferroni and Benjamini-Hochberg methods.](#)²³ The KEGG / Biocarta pathways enrichment scores were calculated by combining

four methods including Significance Analysis of Microarray to Gene-Set Analysis (SAM-GS), Gene Set Analysis (GSA), and globaltest. The median score across the four methods was used to rank the pathways. Methodological details are given in the Supplementary Materials and Methods (Method S1). Raw gene expression data have been deposited to ArrayExpress under accession number E-TABM-702.

Array-based comparative genomic hybridization (aCGH)

Genome analyses of eight NKTCLs, SNK6 and SNT8 cell lines were performed using the human genome-wide CIT-CGH array (V6) containing 4434 sequence verified bacterial artificial chromosome (BAC) clones (with quadruplicate spots per clone) with a median gap between two successive clones of 600 kb. The characteristics of this array have been previously reported. aCGH raw data (deposited to ArrayExpress under accession number E-TABM-791) were normalized using the within print-tip group lowess method; smoothing, breakpoints detection and status (Gain/Loss) determination were calculated using the Bioconductor package GLAD. Methodological details are given in the Supplementary Materials and Methods (Method S1).

Immunohistochemistry

Immunohistochemistry was performed on deparaffinized tissue sections using a standard indirect avidin-biotin immunoperoxidase method. After appropriate antigen retrieval, sections were stained for EBI3 (2G4H6);²⁴ pSTAT3 at Tyr705 (D3A7), pAKT at Ser473 (736E11) (Cell Signaling Technology, Danvers, MA); VEGFA (C1), VCAM-1 (E10), cRel (B-6), PDGFR α and pPDGFR α (Santa Cruz Biotechnology, Santa Cruz, CA); E-cadherin (NCH-38, DakoCytomation, Glostrup, Denmark); CD163 (10D6, Novocastra-Leica, Wetzlar, Germany); clusterin (41D, Upstate-Millipore, Billerica, MA); CCND1 (SP4, Lab Vision-Thermo Fisher

Scientific, Fremont, CA); epidermal growth factor receptor (EGFR) (31G7, Zymed-Invitrogen, Carlsbad, CA); β -catenin (14, BD Biosciences, Erembodegem, Belgium); RelB (EP613Y, Epitomics, Burlingame, CA). For granzyme H (gzm H) (4G5)²⁵ and RelA (Santa Cruz Biotechnology), tyramide signal amplification system (CSAII kit, DakoCytomation) and peroxidase-labeled dextran polymer (EnVision+, DakoCytomation) were applied, respectively. Adequate control tissues for specific antibodies were included.

Quantitative reverse-transcriptase PCR analysis of candidate genes

The expression of candidate genes (*HACE1*, *CCL2*, *TNFRSF21*, *CCND3*, *MET*) identified in altered chromosomal regions was determined by TaqMan[®] quantitative reverse-transcriptase PCR (qRT-PCR) (Applied Biosystems, Foster City, CA) in six primary tumors, three NKTCL cell lines and in resting normal NK cells as control. The expression of *HACE1* was compared to that of *PRDM1*, *ATG5* and *AIM1*, three candidate tumor suppressor genes in NKTCL also mapping at 6q21.⁵ All primers and probes were purchased from Applied Biosystems and the gene expression was measured using Mastercycler[®] ep realplex^{2S} system (Eppendorf, Hamburg, Germany). Quantifications were done in duplicate and mean values and standard deviation were calculated for each transcript as previously described.²⁶

PDGFRA gene analysis

PDGFRA gene analysis was performed in six primary tumors and in three cell lines. *PDGFRA* copy numbers in intron 1 (Syst: Hs05935655_cn,hg18.v7) and exons 7-8 (Syst: Hs04818823_cn,hg18.v7) were measured on a LightCycler 480 (Roche Diagnostics, Meylan, France), using TaqMan[®] copy number assays according to the manufacturer's instructions (Applied Biosystems). *ALB* gene was used as the reference gene.²⁷

The mutations of *PDGFRA* exons 12, 14 and 18 were searched by Length Analysis of PCR Products (LAPP) and sequencing as described previously.²⁸

To search for mutations and polymorphisms in the *PDGFRA* promoter region, genomic DNA was amplified by PCR using the primers 1651F and 727R as described by Toepoel et al.²⁹. After purification (PCR purification kit, GE Healthcare, Freiburg, Germany), automated sequencing was performed on the ABI310 genetic analyzer with the Big Dye terminator sequencing kit (Applied Biosystems) using the primers 1562F, 1340R, 1110F, and 759R (see supplementary data). Sequences were compared to the reference sequence for *PDGFRA* promoter (GenBank accession number X80389).

³H thymidine-labeled proliferation assay

Cells were washed extensively to remove IL-2 and plated at 20,000 cells per well, in the presence or absence of imatinib mesylate (Axon Medchem BV, Groningen, The Netherlands), at 3 different concentrations (1, 3, and 6 μ M) and incubated for 72 hours. One μ Ci of tritium thymidine was added 6 hours before evaluating the proliferation using Packard TopCount Liquid Scintillation Counter (GMI, Ramsey, MN). Results were expressed as the percentage of proliferation measured in the absence of inhibitor. All experiments were performed in triplicate.

RESULTS

The molecular signature of NKTCL differs from that of normal NK cells

The Affymetrix expression profiles of seven NKTCL samples were compared with those of normal NK cells (n=6). A total of 2447 and 2339 probe sets corresponding to 1721 and 1436 overexpressed and underexpressed genes, respectively, significantly distinguished NKTCL tissues from normal NK cells ($P < 0.005$) (Tables 2 and S1). As expected, genes related to the

microenvironment, notably macrophages (*CLU*, *CD68*, *CD163*) were among the most differentially overexpressed in NKTCL tissues. As shown in Tables 2 and S1, the other genes overexpressed in NKTCL tissues included genes involved in the autophagy (*ATG3*, *ATG7*) and in the cell cycle control (*CCND1*), related to cell-to-cell interactions (*CDH1*, *ITGA7*, *ITGA9*, *ITGB4*, *VCAM1*), chemokines (*CX3CLI*, *CXCL9*, *CXCL10*), cytokines (*IL8*, *IL20*, *IL33*), extracellular matrix (ECM) interactions (*MMP11*, *MMP14*, *TIMP1*, *TIMP2*, *TIMP3*), innate immunity (*IL411*, *TLR4*, *TLR7*, *TLR8*), local invasion and metastasis (*COL1A1*, *COL1A2*, *FNI*, *LAMB1*), angiogenesis (*ANGPT2*, *VEGFA*, *VEGFB*, *VEGFC*, *KDR*), growth factors and their receptors (*PDGFRA*, *PDGFB*, *PDGFC*, *TGFB2*, *TGFB3*), oncogenes (*MAFB*, *MET*, *MYC*) and genes reported to be induced by EBV in vitro (*CDH1*, *EBI3*, *BASPI*, *DNASE1L3*, *HCK*, *HLA-DQA1*, *IFI30*, *IFI44L*, *IFITM3*, *LGALS9*, *THRA*, *TNFRSF10D*).^{15,30} *PCDH15*, a gene previously shown to be specifically expressed in NKTCLs³¹ was also overexpressed, albeit with less statistical significance. Some of these genes were also overexpressed in SNK6 and SNT8 cell lines compared to normal NK cells, for example, *VCAM1*, *CXCL10*, *EBI3*, *TIMP1*, *MYC*, *PDGFRA*, *KDR* and *VEGFA* (Tables 2 and S1). Interestingly, NKTCL appeared to be more closely related to activated than to resting NK cells, as the level of expression of about two-thirds of the NKTCL signature was closer to that of activated NK cells than that of resting NK cells.

Among these overexpressed genes tested by immunohistochemistry, E-cadherin, CD163, clusterin, EGFR, and cyclin D1 expression was restricted to non-neoplastic cells, i.e. epithelial cells (E-cadherin, clusterin, cyclin D1, EGFR), stromal cells (clusterin, cyclin D1) and numerous histiocytes (CD163) (Table 3). By contrast, VCAM1 and the EBV-induced gene 3 (EBI3), a subunit of IL-27, labeled the neoplastic cells of 4/13 (31%) and 9/12 (75%) evaluable NKTCLs, respectively (Figure 1B). SNK6 and MEC04 cells were also positive for EBI3.

NKTCL has a distinct molecular signature compared to PTCL, NOS

Unsupervised, consensus clustering applied to the molecular signatures of nine NKTCL samples (seven biopsies and two cell lines) and 16 PTCL, NOS samples, generated two main branches correlated to the pathological diagnosis. Indeed, all NKTCL samples clustered in one branch, and the other branch comprised PTCL, NOS cases only (Figure 2). Interestingly, one case of nodal $\gamma\delta$ PTCL, NOS with an activated cytotoxic profile (gzm B+) but negative for EBV (sample C2) clustered with NKTCL cases.

By supervised analysis, a total of 372 and 691 probe sets corresponding to 278 and 484 overexpressed and underexpressed genes, respectively, significantly distinguished tissues involved by NKTCLs versus PTCLs, NOS ($P < 0.005$) (Tables 4 and S2). As expected, among the top overexpressed genes in NKTCLs were many genes encoding KIRs, and others encoding NK-cell associated molecules (*NCAM1*, *CD244*) or related to cytotoxic functions (*GZMB*, *GZMH*, *CTSW*, *PRF1*...). Significantly, NKTCLs also overexpressed genes encoding cell adhesion molecules (*ITGAM*, *ITGB6*), chemokines and their receptors (*CCLA*, *CCL5*, *CCR1*), apoptosis-related molecules (*FASLG*, *BCL2L2*), cytidine deaminase (*APOBEC3G*), and oncogenes (*MYC*, *RHOC*). In addition to NCAM1 (CD56) and cytotoxic proteins such as TiA1 and gzm B which were strongly expressed in all NKTCLs, we investigated the expression of another cytotoxic granule-associated protein, gzm H, of which transcript levels were 13.66 times higher than in PTCLs, NOS. As shown in figure 1, a strong granular cytoplasmic staining was found in virtually all neoplastic cells of all NKTCL tumors tested (n=16) as well as in the SNK6 and MEC04 cells whereas gzm H was restricted to small lymphocytes in most PTCLs, NOS. Among PTCL, NOS, the $\gamma\delta$ T-cell lymphoma was gzm H positive and another case disclosed heterogeneous partial staining.

Patterns of copy number aberrations and identification of genes relevant to the pathobiology of NKTCL

The aCGH findings are summarized in Table 5 and in Figure 3. Extensive losses and gains of larger and smaller chromosomal regions were found in all NKTCL samples analyzed. Recurrent copy number aberrations (CNA) observed in $\geq 3/8$ (37.5%) NKTCL biopsy samples, comprised 16 regions of chromosomal gains (on 10p15, 7q35-q36, 7p11.2-p12, 7q11.2-q34, 16p13.3, 17q12 and on 1q21-q44, 4p16, 6p11.1-p25, 6q11.1-q14, 6q27, 8p23.3, 9q34, 10p14-p15, 11p15, and 22q11.21) and four regions of losses (on 6q16-q25, 11q24-q25, 17p13.3, and 8p22-p23).

To identify candidate genes in the regions of CNA, we selected the genes with a Welch's T-test *P*-value less than 0.001 and a fold average expression difference > 2.0 (or < 0.5) in NKTCL tissues compared to normal NK cells. The resulting list (Table S3) included genes related to malignant transformation and invasion (*SI00A16*, *LAMBI*, *LAMC1*, *COL1A2*, *CTSB*), cell cycle progression (*CCND3*), signal transduction (*FYN*), tumor suppressor genes (*HACE1*, *CAV1*, *CAV2*, *DLC1*), as well as members of important pathways which, according to GEP analysis, appear deregulated in NKTCL (see below), such as angiogenesis (*MET*, *SI00A13*), NF- κ B (*PRKCQ*, *TNFRSF21*), WNT (*CUL1*, *FZD1*, *SGK1*), and JAK-STAT (*AKT3*, *IL6R*, *CCL2*) signaling pathways.

We selected for qRT-PCR correlation several biologically relevant deregulated candidate genes mapping to altered chromosomal regions at 6q21 (*HACE1*), 17q12 (*CCL2*), 6p12.3 (*TNFRSF21*), 6p21.1 (*CCND3*), 7q31.2 (*MET*). We also evaluated *ATG5*, *AIM1*, *PRDMI* genes reported as candidate tumor suppressor genes at 6q21 in NKTCL cell lines, that were downexpressed in our microarray data albeit at less statistical significance. In agreement with the microarray results, we confirmed by qRT-PCR the overexpression of *MET*, *CCL2*, *TNFRSF21* in NKTCL samples compared to normal NK cells and the

underexpression of *CCND3* and *HACE1* (Figure 4). *ATG5* and *AIM1* transcripts were also markedly reduced in both cell lines and primary tumors. In contrast, quantification of *PRDM1* mRNA gave discrepant results in cell lines (underexpressed levels, in accordance with published data⁵) and primary tumors (increased transcript levels in four of six samples). These findings were independent of the presence or absence of 6q21 deletion.

Identification of distinct pathways in NKTCL

In order to identify potentially relevant biological pathways in NKTCL, four gene sets analysis methods were applied. The most discriminatory pathways when comparing NKTCL and normal NK cells or PTCL, NOS, comprised those related to important cell functions such as apoptosis, cell adhesion, cell communication, ECM-receptor interaction, cell cycle (p27 regulation), cytokine-cytokine receptor interaction, as well as TGF β , MAPK, WNT and JAK-STAT signalling pathways (Table 6, Figure 5A and E). More specifically, angiogenesis-related (VEGF) and NF- κ B were also discriminatory pathways between neoplastic samples and normal NK cells. FAS and AKT signaling genes pathways and especially genes related to NK-cell mediated cytotoxicity (Figure 5B, C, D, and F) were differentially expressed between NKTCL and PTCL, NOS.

For example, as illustrated in Figure 5A, several component genes of JAK-STAT pathway like *IL13RA1*, *IL6R*, *STAT1*, *STAT2*, *VEGFA*, *CCND1* and *MYC* were overexpressed in NKTCL compared to normal NK cells and *IL12RB1*, *IL20*, *IL2RB*, and *MYC* compared to PTCL, NOS. Altogether, the pathway analysis supports the involvement of several important pathways in NKTCL.

Activation of several oncogenic pathways (AKT, STAT3, NF- κ B, VEGF) in NKTCL

In order to evaluate the possible activation of pathways identified using statistical methods, the expression of several representative genes was assessed at the protein level (Table 3 and Figure 1). Nuclear expression of phosphorylated AKT (Ser473) and STAT3 (Tyr705) was found in 9/9 and 13/14 NKTCL cases, respectively. Strong expression of VEGFA, one of the important STAT3-regulated gene products related to angiogenesis and immune evasion,³² was demonstrated in 9/9 NKTCL and expression of its receptor VEGFR2 was evidenced in the neoplastic cells of 4/5 tumors. Positivity for pSTAT3 and VEGFA was confirmed in MEC04 and SNK6 cell lines, and pAKT was demonstrated in MEC04 cells.

Differential expression of WNT and NF- κ B pathway genes were also identified in pathway analyses. Nuclear expression of β -catenin, a hallmark of activation of WNT pathway, was not observed in neoplastic cells (n=8), contrasting with cytoplasmic and/or membrane staining in surrounding epithelial and endothelial cells. On the other hand, RelA and cRel, two important molecules of the canonical NF- κ B pathway, were expressed in the cytoplasm of most evaluable NKTCLs associated with nuclear localization of RelA (Figure 1). RelB, a molecule of the alternative NF- κ B pathway, was negative in all investigated NKTCLs (n=6).

Activation of PDGFRA pathway in NKTCL

Since PDGFR α , a receptor tyrosine kinase mediating important cell functions such as migration, proliferation and cell survival and known to interact with PI3K/AKT and STAT proteins,³³ was highly expressed at the mRNA level (Table 2 and Figure 5B), this factor was evaluated by immunohistochemistry. Eleven of 13 (85%) NKTCL cases showed cytoplasmic expression of PDGFR α . In addition, its phosphorylated form (pPDGFR α) was found in all 13 NKTCLs (Table 3 and Figure 1). In agreement with a recent report,³⁴ expression of both PDGFR α and pPDGFR α was also demonstrated in most PTCLs, NOS (Table 3). In view of

these findings, we investigated the potential implication of the PDGF signaling pathway in the proliferation of NKTCL cells. Imatinib mesylate induced dramatic concentration-dependent growth inhibition of PDGFR α -positive MECO4 cells whereas the effect on SNK6 cells was minimal. As shown in Figure 6, a significant 50% growth inhibition was already observed when MECO4 cells were exposed to imatinib mesylate at 1 μ M that increased to 90% at 6 μ M. U937 used as a control cell line known to be resistant to imatinib mesylate maintained 63 % proliferation with 6 μ M imatinib.

We further searched for potential genetic alterations underlying *PDGFRA* deregulation. The absence of copy number gain in *PDGFRA* locus validated by real-time PCR in eight interpretable samples was concordant with the absence of genomic imbalance in 4q11-q13 observed in our BAC array CGH data. In addition, we did not evidence mutations in exons 12, 14 and 18 of *PDGFRA*, in agreement with previous findings.³⁵

Finally, we performed mutations and polymorphisms analysis within the *PDGFRA* promoter region and in particular investigated the distribution of haplotypes which have been reported in association with different transcriptional activities.³⁶ Sequence analysis did not show any mutation in the nine samples tested (compared to the reference sequence), and the distribution in the haplotypes - four samples had a H1/H2 α genotype, three H2 α /H2 α , one H2 α /H2 β and one H2 α /H2 γ – corresponded to that reported in the Western European population (see supplementary data).

DISCUSSION

In the present study, we characterized the molecular signature of NKTCL in comparison to normal NK cells and to PTCL, NOS. This led to the identification of deregulated genes and signaling pathways which might be relevant to the pathophysiology and clinicopathologic features of the disease and bring rationale for the development of new therapies.

Unsupervised clustering remarkably segregated NKTCL and PTCL, NOS samples. Notably, the NKTCL case with a T-cell cytotoxic phenotype (sample T5) clustered with those of NK cell origin, providing another molecular argument for grouping nasal “true NK-” and cytotoxic T-cell lymphomas as a single entity as proposed in the current WHO classification.¹ Interestingly, the NKTCL case of T-cell derivation also showed the 6q16-q25 deletion. The only mismatch was represented by one PTCL, NOS in the NKTCL cluster. That particular case had a $\gamma\delta$ activated cytotoxic phenotype suggesting that derivation from the innate immune system might imprint a peculiar signature.³⁷

By comparison to PTCL, NOS, the molecular signature of NKTCL was significantly contributed by an overexpression of genes associated with cytotoxic functions and NK-cell-associated molecules. Interestingly, the highest fold change of expression was observed for *gzm H* transcripts. Granzyme H, a *gzm* family member sharing a 90% amino acid sequence identity with *gzm B*, is constitutively expressed in NK cells irrespective of their activation status²⁵ but acts differently from *gzm B* by inducing a caspase-independent cell death program.³⁸ We confirmed a strong *gzm H* protein expression in all NKTCLs contrasting with its negativity in most PTCLs, NOS, with the notable exception of the $\gamma\delta$ T-cell lymphoma. Therefore, *gzm H* appears to be a novel sensitive marker for NKTCL, although its specificity needs to be delineated with respect to its possible expression in other lymphomas derived from the innate immune system.

Other aspects of the NKTCL signature could be related to some peculiar clinicopathologic features of the disease. Angioinvasion and angiocentricity typical of NKTCL, might be accounted by the high expression of genes such as *VCAMI*, *CXCL9*, and *CXCL10*, encoding proteins involved in the interaction with endothelium or in the pathogenesis of tissue necrosis and vascular damage associated with EBV-positive lymphoproliferations.³⁹ NKTCL, which in most instances arises in the nasal area, is also

characterized by a strong tendency to disseminate to other extranodal distant sites. In view of the known roles of CCR7 and SELL/CD62L in peripheral lymph node homing and that of CCL27, CXCL12, in homing to the skin, intestine and bone marrow, it is likely that the lower levels of CCR7 and SELL/CD62L and the overexpression of CXCL12 might explain the pattern of distribution of the disease.

We confirmed here recurrent genomic gains and losses previously reported in NKTCL. Deletion of chromosome 6q reported as the most characteristic but not specific genetic alteration in NKTCL,^{3-5,40-42} was present in 40% of our cases, including SNK6 cell line. In line with the recent report by Iqbal et al., we also found recurrent gain of 1q21-q44 and loss of 17p13.3 in primary tumor samples.⁵ These authors found *PRDMI*, *ATG5*, and *AIMI* as target genes in the region of del6q21 and reported both mutation and methylation in *PRDMI*. Here, we further extended these previous findings by showing low levels of *ATG5* and *AIMI* transcripts in primary tumors. Conversely, *PRDMI* showed a wide range of expression from case to case. In addition, we also found marked reduction in transcripts of *HACE1*, a gene encoding a novel E3 ubiquitin ligase, which is the target of epigenetic inactivation in Wilms' tumor and has been proposed as a tumor suppressor gene in multiple human cancers. *Hace1*^{-/-} mice are spontaneously prone to developing multiple malignant tumors in various organs.⁴³ Taken together, it is therefore tempting to speculate that *HACE1* might be also involved in the pathogenesis of NKTCL.

The proto-oncogene *MET* mapping in 7q31, a region of recurrent gain in our series, was overexpressed in our samples. This receptor with tyrosine-kinase activity is a receptor to HGF, also overexpressed at the mRNA level in our NKTCL series. Interestingly, this pair of ligand-receptor appears to be linked to angiogenesis, tumor formation, invasion, and metastasis.⁴⁴ These findings, together with the expression of VEGFA and its receptor

VEGFR2 might reflect the implication of angiogenesis and/or VEGF signaling pathway in the pathophysiology of NKTCL.

The molecular pathways involved in the pathogenesis of NKTCL are largely unknown. Our study identified deregulated pathways in NKTCL, in comparison to normal NK cells and PTCL, NOS. Among growth factor receptors, the receptor tyrosine kinase PDGFR α was expressed at a higher level than in normal NK cells, both at the mRNA and protein levels, in its activated phosphorylated form, a feature which appears to be shared with PTCL, NOS.³⁴ PDGF signaling pathway is known to be associated with both JAK-STAT and AKT pathways. The AKT protein kinases play a critical role in cell proliferation, survival and programmed cell death, transcription, and cell migration via phosphorylation of a multitude of substrates. Signal transducers and activators of transcription (STATs) are transcription factors activated in response to cytokines and growth factors. STAT3 in particular plays a crucial role in regulating cell growth and apoptosis.³² Several solid or hematological malignancies including ALK-positive anaplastic large cell lymphomas show constitutive STAT3 activation. Using statistical methods, we showed here that AKT and JAK-STAT pathways were differentially expressed in comparison to normal NK cells and/or PTCL, NOS. In addition, we evidenced the nuclear expression of the phosphorylated forms of STAT3 and AKT in most NKTCLs implying constitutive activation of these pathways in this disease. Our results expand recent findings that AKT was phosphorylated in NK-92 cell line and in a few NKTCL primary tumors, probably through involvement of IL-2 or IL-15.⁴⁵ Many genes related to proliferation and survival, angiogenesis, and immunosuppression are known to be regulated by STAT3.³² The high transcript levels of several genes regulated by STAT3 in NKTCL compared to normal NK cells such as *MYC*, *VEGFA*, *BCL2L1*, - and also less significantly *BIRC5*, *HGF*, *IL6*, *MMP2*, *MMP9*, *IL10*, and *CDK5* - suggests its implication in the pathogenesis of NKTCL. Among these, MMP2, MMP9 and IL-10 proteins have already been

evidenced in NKTCL tumor cells and we show here immunohistochemical expression of VEGFA.^{46,47} Recently, we demonstrated that the inhibition of STAT3 activation leads to underexpression of two STAT3 target gene products, BCL-X_L and MYC in MEC04 cells.¹⁷ Altogether, these data provide strong arguments supporting the involvement of JAK-STAT and AKT pathways in NKTCL (Figure 7).

EBV, constantly present in NKTCL, is suspected to play an important role in oncogenesis. Here we showed that, in comparison to EBV-negative normal NK cells, NKTCL overexpressed several EBV-induced genes.^{15,30} In agreement with a previous report,²⁴ one of these genes, *EBI3*, was validated at the protein level. Among the various mechanisms involved in NF- κ B pathway, EBV is known to activate NF- κ B pathway through LMP-1 and/or TRAF,⁴⁸ especially in Hodgkin lymphoma and in EBV-positive B-cell lymphoproliferative disorders. Here, we showed differential expression of this pathway in NKTCL and further demonstrate expression of RelA, supporting activation of NF- κ B in this entity. Interestingly, *TNFAIP3* gene, encoding an inhibitor of the NF- κ B pathway, maps to the region of recurrent loss in 6q16-q25 and was underexpressed in our study. Deletions and/or somatic mutations of this gene have been recently reported in classical Hodgkin lymphoma and primary mediastinal B-cell lymphoma as well as in MALT lymphoma^{49,50} supporting the role of this key regulator of NF- κ B activity as a novel tumor suppressor gene in these lymphomas. Altogether, these findings suggest the involvement of NF- κ B pathway in the pathogenesis of NKTCL. The respective role of EBV and/or *TNFAIP3* inactivation in NF- κ B activation in NKTCL needs further investigation.

The demonstration of pPDGFR α by immunohistochemistry prompted us to test the sensitivity of NKTCL cell lines *in vitro* to imatinib mesylate. The effect of the drug already significant at a 1 μ M concentration with a 50% growth inhibition on MEC04 cells, was most prominent (90% inhibition of growth) at 6 μ M. Conversely, there was no substantial cytotoxic

effect on the SNK6 cell line, which might be related to a lower expression of *PDGFRA*, as suggested at the RNA level (Figure 3). Although our results do not preclude the precise mechanism of action of imatinib and suggest heterogeneity in the sensitivity to the drug, the dramatic effect on MEC04 cells shed light on the possible use of tyrosine kinase inhibitors as a novel therapeutic option in some patients with NKTCL refractory to conventional therapies.

The cause of *PDGFRA* deregulation in NKTCL remains to be determined. We did not evidence either genomic imbalances or gene mutations. Furthermore, mutations in the promoter region were absent in NKTCL primary tumors and cell lines, and we did not find overrepresentation of H2 α haplotype, known to result in upregulation of *PDGFRA* in glioblastoma.²⁹

In conclusion, this integrative genomic and transcriptomic study characterizes the molecular signature of NKTCL, highlights emerging oncogenic pathways in this disease entity and offers rationale for exploring new therapeutic options such as tyrosine kinase inhibitors in patients with this aggressive malignancy.

ACKNOWLEDGEMENTS

This work is part of the Carte d'Identité des Tumeurs (CIT) program (<http://cit.ligue-cancer.net/index.php/en>) from the Ligue Nationale Contre le Cancer. This work was supported by the Institut National de la Santé et de la Recherche Médicale (INSERM), the Institut National du Cancer (INCa), the Belgian National Fund for Scientific Research (FNRS), and the Association pour la Recherche Thérapeutique, Génétique et Immunologique dans les Lymphomes (ARTGIL). Y.H. was supported by the Ligue Nationale Contre le Cancer. We are extremely thankful for the contributions made by the CIT platforms (Affymetrix - IGBMC: Christelle Thibault, Philippe Kastner; BAC arrays - Institut Curie: Gaëlle Pierron, Olivier Delattre; RNA analysis – Saint-Louis hospital: Daniela Geromin). We

also thank [Norio Shimizu for providing cell lines](#), Joe A. Trapani and Odile Devergne for providing antibodies, François Radvanyi for critical opinion in data interpretation, Marie-Laure Prunet from GELAP, Virginie Fataccioli, Tony Noel, Yolaine Pothin and Maryse Baia for technical assistance.

AUTHORSHIP:

Contribution: L.d.L and P.G. designed research; Y.H., A.d.R., B.G., N.M-G., P.C., M-H.D-L., J-F.E., M.T. and C.S. performed research; Y.H., A.d.R., and P.G. analyzed and interpreted the data; L.d.L., Ja.B., J.B., B.P., and P.G. collected data; A.d.R., E.T. and T.M. contributed vital analytical tools; Y.H., A.d.R., L.d.L., P.C., C.S. and P.G. drafted the manuscript.

Conflict-of-interest disclosure: The authors declare no competing financial interests.

Correspondence: Philippe Gaulard, MD, Département de Pathologie and Inserm U955, Hôpital Henri Mondor, 94010 Créteil, France; e-mail : philippe.gaulard@hmn.aphp.fr.

REFERENCES:

1. Swerdlow SH, Campo E, Harris NL, et al. WHO classification of tumours of the haematopoietic and lymphoid tissues. Lyon: International Agency of Research on Cancer (IARC); 2008.
2. Haedicke W, Ho FC, Chott A, et al. Expression of CD94/NKG2A and killer immunoglobulin-like receptors in NK cells and a subset of extranodal cytotoxic T-cell lymphomas. *Blood*. 2000;95:3628-3630.
3. Nakashima Y, Tagawa H, Suzuki R, et al. Genome-wide array-based comparative genomic hybridization of natural killer cell lymphoma/leukemia: different genomic alteration patterns of aggressive NK-cell leukemia and extranodal Nk/T-cell lymphoma, nasal type. *Genes Chromosomes Cancer*. 2005;44:247-255.
4. Ko YH, Choi KE, Han JH, Kim JM, Ree HJ. Comparative genomic hybridization study of nasal-type NK/T-cell lymphoma. *Cytometry*. 2001;46:85-91.
5. Iqbal J, Kucuk C, Deleeuw RJ, et al. Genomic analyses reveal global functional alterations that promote tumor growth and novel tumor suppressor genes in natural killer-cell malignancies. *Leukemia*. 2009;23:1139-1151.
6. Feldman AL, Law M, Grogg KL, et al. Incidence of TCR and TCL1 Gene Translocations and Isochromosome 7q in Peripheral T-Cell Lymphomas Using Fluorescence In Situ Hybridization. *Am J Clin Pathol*. 2008;130:178-185.
7. Kuo TT, Shih LY, Tsang NM. Nasal NK/T cell lymphoma in Taiwan: a clinicopathologic study of 22 cases, with analysis of histologic subtypes, Epstein-Barr virus LMP-1 gene association, and treatment modalities. *Int J Surg Pathol*. 2004;12:375-387.

8. Kim TM, Park YH, Lee SY, et al. Local tumor invasiveness is more predictive of survival than International Prognostic Index in stage I(E)/II(E) extranodal NK/T-cell lymphoma, nasal type. *Blood*. 2005;106:3785-3790.
9. Bossard C, Belhadj K, Reyes F, et al. Expression of the granzyme B inhibitor PI9 predicts outcome in nasal NK/T-cell lymphoma: results of a Western series of 48 patients treated with first-line polychemotherapy within the Groupe d'Etude des Lymphomes de l'Adulte (GELA) trials. *Blood*. 2007;109:2183-2189.
10. Armitage J, Vose J, Weisenburger D. International peripheral T-cell and natural killer/T-cell lymphoma study: pathology findings and clinical outcomes. *J Clin Oncol*. 2008;26:4124-4130.
11. Takakuwa T, Dong Z, Nakatsuka S, et al. Frequent mutations of Fas gene in nasal NK/T cell lymphoma. *Oncogene*. 2002;21:4702-4705.
12. Quintanilla-Martinez L, Kremer M, Keller G, et al. p53 Mutations in nasal natural killer/T-cell lymphoma from Mexico: association with large cell morphology and advanced disease. *Am J Pathol*. 2001;159:2095-2105.
13. Yamaguchi M, Kita K, Miwa H, et al. Frequent expression of P-glycoprotein/MDR1 by nasal T-cell lymphoma cells. *Cancer*. 1995;76:2351-2356.
14. Lin CW, Chen YH, Chuang YC, Liu TY, Hsu SM. CD94 transcripts imply a better prognosis in nasal-type extranodal NK/T-cell lymphoma. *Blood*. 2003;102:2623-2631.
15. Zhang Y, Ohyashiki JH, Takaku T, Shimizu N, Ohyashiki K. Transcriptional profiling of Epstein-Barr virus (EBV) genes and host cellular genes in nasal NK/T-cell lymphoma and chronic active EBV infection. *Br J Cancer*. 2006;94:599-608.
16. Nagata H, Konno A, Kimura N, et al. Characterization of novel natural killer (NK)-cell and gammadelta T-cell lines established from primary lesions of nasal T/NK-cell lymphomas associated with the Epstein-Barr virus. *Blood*. 2001;97:708-713.
17. Coppo P, Gouilleux-Gruart V, Huang Y, et al. STAT3 transcription factor is constitutively activated and is oncogenic in nasal-type NK/T-cell lymphoma. *Leukemia*. 2009;23:1667-1678.
18. de Leval L, Rickman DS, Thielen C, et al. The gene expression profile of nodal peripheral T-cell lymphoma demonstrates a molecular link between angioimmunoblastic T-cell lymphoma (AITL) and follicular helper T (TFH) cells. *Blood*. 2007;109:4952-4963.
19. Dybkaer K, Iqbal J, Zhou G, et al. Genome wide transcriptional analysis of resting and IL2 activated human natural killer cells: gene expression signatures indicative of novel molecular signaling pathways. *BMC Genomics*. 2007;8:230.
20. Caron G, Le Gallou S, Lamy T, Tarte K, Fest T. CXCR4 expression functionally discriminates centroblasts versus centrocytes within human germinal center B cells. *J Immunol*. 2009;182:7595-7602.
21. Compagno M, Lim WK, Grunn A, et al. Mutations of multiple genes cause deregulation of NF-kappaB in diffuse large B-cell lymphoma. *Nature*. 2009;459:717-721.
22. de Reynies A, Assie G, Rickman DS, et al. Gene expression profiling reveals a new classification of adrenocortical tumors and identifies molecular predictors of malignancy and survival. *J Clin Oncol*. 2009;27:1108-1115.
23. Strimmer K. A unified approach to false discovery rate estimation. *BMC Bioinformatics*. 2008;9:303.
24. Larousserie F, Bardel E, Pflanz S, et al. Analysis of interleukin-27 (EBI3/p28) expression in Epstein-Barr virus- and human T-cell leukemia virus type 1-associated lymphomas: heterogeneous expression of EBI3 subunit by tumoral cells. *Am J Pathol*. 2005;166:1217-1228.
25. Sedelies KA, Sayers TJ, Edwards KM, et al. Discordant regulation of granzyme H and granzyme B expression in human lymphocytes. *J Biol Chem*. 2004;279:26581-26587.

26. Travert M, Ame-Thomas P, Pangault C, et al. CD40 ligand protects from TRAIL-induced apoptosis in follicular lymphomas through NF-kappaB activation and up-regulation of c-FLIP and Bcl-xL. *J Immunol.* 2008;181:1001-1011.
27. Pongers-Willemse MJ, Verhagen OJ, Tibbe GJ, et al. Real-time quantitative PCR for the detection of minimal residual disease in acute lymphoblastic leukemia using junctional region specific TaqMan probes. *Leukemia.* 1998;12:2006-2014.
28. Tabone-Eglinger S, Subra F, El Sayadi H, et al. KIT mutations induce intracellular retention and activation of an immature form of the KIT protein in gastrointestinal stromal tumors. *Clin Cancer Res.* 2008;14:2285-2294.
29. Toepoel M, Joosten PH, Knobbe CB, et al. Haplotype-specific expression of the human PDGFRA gene correlates with the risk of glioblastomas. *Int J Cancer.* 2008;123:322-329.
30. Carter KL, Cahir-McFarland E, Kieff E. Epstein-barr virus-induced changes in B-lymphocyte gene expression. *J Virol.* 2002;76:10427-10436.
31. Rouget-Quermalet V, Giustiniani J, Marie-Cardine A, et al. Protocadherin 15 (PCDH15): a new secreted isoform and a potential marker for NK/T cell lymphomas. *Oncogene.* 2006;25:2807-2811.
32. Yu H, Kortylewski M, Pardoll D. Crosstalk between cancer and immune cells: role of STAT3 in the tumour microenvironment. *Nat Rev Immunol.* 2007;7:41-51.
33. Andrae J, Gallini R, Betsholtz C. Role of platelet-derived growth factors in physiology and medicine. *Genes Dev.* 2008;22:1276-1312.
34. Piccaluga PP, Agostinelli C, Califano A, et al. Gene expression analysis of peripheral T cell lymphoma, unspecified, reveals distinct profiles and new potential therapeutic targets. *J Clin Invest.* 2007;117:823-834.
35. Chen YP, Chang KC, Su WC, Chen TY. The expression and prognostic significance of platelet-derived growth factor receptor alpha in mature T- and natural killer-cell lymphomas. *Ann Hematol.* 2008;87:985-990.
36. Joosten PH, Toepoel M, Mariman EC, Van Zoelen EJ. Promoter haplotype combinations of the platelet-derived growth factor alpha-receptor gene predispose to human neural tube defects. *Nat Genet.* 2001;27:215-217.
37. Krenacs L, Smyth MJ, Bagdi E, et al. The serine protease granzyme M is preferentially expressed in NK-cell, gamma delta T-cell, and intestinal T-cell lymphomas: evidence of origin from lymphocytes involved in innate immunity. *Blood.* 2003;101:3590-3593.
38. Fellows E, Gil-Parrado S, Jenne DE, Kurschus FC. Natural killer cell-derived human granzyme H induces an alternative, caspase-independent cell-death program. *Blood.* 2007;110:544-552.
39. Teruya-Feldstein J, Jaffe ES, Burd PR, et al. The role of Mig, the monokine induced by interferon-gamma, and IP-10, the interferon-gamma-inducible protein-10, in tissue necrosis and vascular damage associated with Epstein-Barr virus-positive lymphoproliferative disease. *Blood.* 1997;90:4099-4105.
40. Taborelli M, Tibiletti MG, Martin V, Pozzi B, Bertoni F, Capella C. Chromosome band 6q deletion pattern in malignant lymphomas. *Cancer Genet Cytogenet.* 2006;165:106-113.
41. Siu LL, Wong KF, Chan JK, Kwong YL. Comparative genomic hybridization analysis of natural killer cell lymphoma/leukemia. Recognition of consistent patterns of genetic alterations. *Am J Pathol.* 1999;155:1419-1425.
42. Sun HS, Su IJ, Lin YC, Chen JS, Fang SY. A 2.6 Mb interval on chromosome 6q25.2-q25.3 is commonly deleted in human nasal natural killer/T-cell lymphoma. *Br J Haematol.* 2003;122:590-599.

43. Zhang L, Anglesio MS, O'Sullivan M, et al. The E3 ligase HACE1 is a critical chromosome 6q21 tumor suppressor involved in multiple cancers. *Nat Med.* 2007;13:1060-1069.
44. Comoglio PM, Giordano S, Trusolino L. Drug development of MET inhibitors: targeting oncogene addiction and expedience. *Nat Rev Drug Discov.* 2008;7:504-516.
45. Chow C, Liu AY, Chan WS, Lei KI, Chan WY, Lo AW. AKT plays a role in the survival of the tumor cells of extranodal NK/T-cell lymphoma, nasal type. *Haematologica.* 2005;90:274-275.
46. Sakata K, Someya M, Omatsu M, et al. The enhanced expression of the matrix metalloproteinase 9 in nasal NK/T-cell lymphoma. *BMC Cancer.* 2007;7:229.
47. Boulland ML, Meignin V, Leroy-Viard K, et al. Human interleukin-10 expression in T/natural killer-cell lymphomas: association with anaplastic large cell lymphomas and nasal natural killer-cell lymphomas. *Am J Pathol.* 1998;153:1229-1237.
48. Jost PJ, Ruland J. Aberrant NF-kappaB signaling in lymphoma: mechanisms, consequences, and therapeutic implications. *Blood.* 2007;109:2700-2707.
49. Chanudet E, Ye H, Ferry J, et al. A20 deletion is associated with copy number gain at the TNFA/B/C locus and occurs preferentially in translocation-negative MALT lymphoma of the ocular adnexa and salivary glands. *J Pathol.* 2009;217:420-430.
50. Schmitz R, Hansmann ML, Bohle V, et al. TNFAIP3 (A20) is a tumor suppressor gene in Hodgkin lymphoma and primary mediastinal B cell lymphoma. *J Exp Med.* 2009;206:981-989.

Table 1. Summary of immunohistochemical, and genotypic features of the NKTCL samples analysed in the study.

Samples	Age	Sex	Biopsy site	CD3ε	CD2	CD5	CD7	CD4	CD8	CD56	TiA1	Gzm B	EBV	T clonality
T1	58	M	Nasopharyngeal region	+	+	-	+	-	-	+	+	+	+	-
T2	25	M	Nasopharyngeal region	+	+	-	-	-	-	+	+	+	+	-
T3	64	M	Skin	+	-	-	ND	-	-	-	+	+	+	-
T4	62	M	Nasopharyngeal region	-	+	-	-	-	-	+	+	+	+	-
T5	72	M	Nasopharyngeal region	+	+	-	-	-	-	+	+	+	+	+
T6	52	F	Nasopharyngeal region	+	+	-	-	ND	-	+	+	+	+	-
T7*	42	M	Hypophysis	+	+	-	-	+	-	+	+	+	+	-
T8†	31	F	Nasopharyngeal region	+	+	-	+	+	ND	+	+	+	+	-
T9†	67	M	Nasopharyngeal region	+	+	-	+	-	+	+	+	+	+	+‡
SNK6	NA	NA	NA	+	+	ND	ND	-	-	+	ND	+	+	-
SNT8	NA	NA	NA	+	+	ND	ND	-	-	+	ND	ND	+	+

*: sample used only for transcriptomic analysis.

†: samples used only for genomic analysis.

‡: this case showed βF1 immunoreactivity on formalin-fixed paraffin-embedded tissues sections, and was negative for δTCR1 on frozen sections.

NA: not applicable.

ND: not done.

Table 2. Selection of genes overexpressed in NKTCL tissues compared to normal NK cells with *P*-value less than 0.005. A complete list of genes is given in the supplementary table S1.

Gene class and specific genes	Fold change
Cell-to-cell interactions	
CDH1 (E-cadherin)*	1.54
ITGA9 (Integrin alpha 9)	2.37
ITGB4 (Integrin beta 4)*	2.15
VCAM1 (Vascular cell adhesion molecule 1)*	26.18
Cell cycle control	
CCND1 (Cyclin D1)*	6.67
Chemokines	
CCL18	10.50
CCL19	80.67
CCL2*	88.11
CCL8*	51.61
CXCL10 (IP10)*	48.07
CXCL12 (SDF-1)	25.75
CXCL9 (Mig)	254.14
Cytokines	
IL13RA1*	9.19
IL6R	2.25
IL33*	2.75
IL8*	5.07
Genes overexpressed in EBV-infected lymphoma cell lines	
EBI3 (EBV induced gene 3)*	2.76
BASP1 (Brain abundant, membrane attached signal protein 1)*	13.21
HCK (Hemopoietic cell kinase)	16.01
TNFRSF10D (Tumor necrosis factor receptor superfamily, member 10d)*	1.53
Extracellular matrix interactions	
COL1A1 (Collagen, type I alpha 1)*	45.91
COL1A2 (Collagen, type I alpha 2)*	33.35
COL3A1 (Collagen, type III alpha 1)*	59.68
FN1 (Fibronectin 1)*	91.79
TIMP1 (TIMP metalloproteinase inhibitor 1)*	6.28
TIMP2 (TIMP metalloproteinase inhibitor 2)	10.79
TIMP3 (TIMP metalloproteinase inhibitor 3)	9.57
Growth factors & receptors	
GHR (Growth hormone receptor)*	1.35
PDGFB (Platelet-derived growth factor beta)*	2.16
PDGFC (Platelet derived growth factor C)*	7.92
PDGFRA (Platelet-derived growth factor receptor, alpha polypeptide)*	7.47
Immunity & lymphocyte development	
CD86*	6.04
HLA-DOA*	12.12
HLA-DRA*	12.18
IL4I1 (Interleukin 4 induced 1)*	6.40
SLAMF8 (SLAM family member 8)*	45.26
TLR2	8.76
TLR7*	5.26
TLR8	13.49
Microenvironment	
CD163	134.47
Oncogenes	
MAFB (V-maf musculoaponeurotic fibrosarcoma oncogene homolog)	37.94
MET (Hepatocyte growth factor receptor)*	2.00
MYC*	1.23
Transcription factors	
STAT1*	5.25

STAT2*	1.86
<hr/>	
Vascular biology	
KDR (VEGFR2)*	1.47
THBD (Thrombomodulin)	4.33
VEGFA*	1.54
VEGFC*	1.68
VWF*	12.97
<hr/>	
Miscellaneous	
AIM2 (Absent in melanoma 2)*	14.76
CD40 (TNF receptor superfamily member 5)*	3.95
FZD1 (Frizzled homolog 1)*	2.55
*: genes are also overexpressed in NKTCL cell lines compared to normal NK cells.	

Table 3. Summary of immunohistochemical results*.

	NKTCL (n=16)	NKTCL cell lines (n=2)	PTCL, NOS (n=17)
Clusterin	0/4 (0%)	0/1	ND
E-cadherin	0/4 (0%)	ND	ND
Cyclin D1	0/4 (0%)	ND	ND
EGFR	0/4 (0%)	ND	ND
CD163	0/4 (0%)	0/2	ND
EBI3	9/12 (75%)	2/2	1/13 (8%)
VCAM1	4/13 (31%)	0/2	0/7 (0%)
Granzyme H	16/16 (100%)	2/2	2/16 (13%)
pSTAT3	13/14 (93%)	2/2 [†]	2/17 (12%)
pAKT	9/9 (100%)	NE	0/16 (0%)
VEGFA	9/9 (100%)	2/2	5/13 (38%)
VEGFR2	4/5 (80%)	2/2 [‡]	ND
PDGFR α	11/13 (85%)	1/1	10/10 (100%)
pPDGFR α	13/13 (100%)	ND	7/8 (88%)
RelA	5/6 (83%) [§]	2/2 [§]	ND
RelB	0/6 (0%)	ND	ND
cRel	4/5 (80%)	0/2	ND
Beta-catenin	0/8 (0%)	ND	ND

*: Results refer to expression in neoplastic cells.

[†]: phosphorylated STAT3 stained most MEC04 cells, but only a minority of SNK6 cells.

[‡]: performed by flow cytometric immunophenotyping.

[§]: cytoplasmic and nuclear staining of neoplastic cells.

^{||}: cytoplasmic staining of most neoplastic cells.

ND: not done.

NE: non evaluable.

Table 4. Selection of genes overexpressed in NKTCL tissues compared to PTCL, NOS cells with *P*-value less than 0.005. A complete list of genes is given in the supplementary table S2.

Gene class and specific genes	Fold change
Apoptosis	
BCL2L2 (BCL-W)	1.68
FASLG (Fas ligand)	5.99
Cell-to-cell interactions	
ITGAM (Integrin, alpha M)	2.30
Chemokines	
CCL4 (MIP-1-beta)	4.30
CCL5 (RANTES)	8.66
Cytokines & receptors	
IL20	1.15
IL2RB	2.32
Growth factors	
TGFB2	1.14
Cytotoxic molecules	
CTSW (Cathepsin W)	11.31
GZMA (Granzyme A)	8.03
GZMB (Granzyme B)	5.39
GZMH (Granzyme H)	13.66
PRF1 (Perforin 1)	3.34
NK cell-associated molecules	
APOBEC3G (Apolipoprotein B mRNA editing enzyme, catalytic polypeptide-like 3G)	2.40
CD244 (NK cell receptor 2B4)	6.75
KIR2DL3 /// KIR2DS5	10.30
KIR2DL4	11.77
KIR2DL5A	7.47
KIR2DS4	4.94
KIR3DL1	9.96
KIR3DL2	14.02
KIR3DL3	12.51
KLRC1 /// KLRC2	25.75
KLRC3	32.96
KLRC4 /// KLRK1	10.33
KLRD1	32.45
NCAM1 (CD56)	10.54
Immune responses	
IRF6 (Interferon regulatory factor 6)	1.54
Oncogenes	
MYC	1.18
RHOC (Ras homolog gene family, member C)	3.22
Transcription factors	
ATF6 (Activating transcription factor 6)	1.39
Miscellaneous	
MAPK1	1.46
PTPN22 (Protein tyrosine phosphatase, non-receptor type 22)	2.47
YWHAH (Tyrosine 3-monooxygenase/tryptophan 5-monooxygenase activation protein, eta polypeptide)	1.62

Table 5. Copy number alterations identified by aCGH in the NKTCL samples analysed in this study.

	Chromosomes	Start position (Mb)	End position (Mb)	No of clones	NKTCL tissues and cell lines (n=10)	NKTCL tissues (n=8)	SNK6	SNT8
GAIN	1q21-q44	143	245	170	5	3	1	1
	4p16	2	6	5	3	3	0	0
	6p25-p11.1	0	58	93	4	3	1	0
	6q11.1-q14	58	87	26	4	3	1	0
	6q27	167	171	5	3	3	0	0
	7p12-p11.2	53	55	4	5	4	0	1
	7q11.2-q34	62	142	99	5	4	1	0
	7q35-q36	143	156	11	6	5	1	0
	8p23.3	0,13	1,96	5	4	3	1	0
	9q34	134	138	7	4	3	1	0
	10p15	0	4	5	6	6	0	0
	10p15-p14	6	8	6	3	3	0	0
	11p15	0	3	10	4	3	1	0
	16p13.3	1	2	5	4	4	0	0
	17q12	28,81	30,78	12	5	3	1	1
	17q12	29,84	30,30	7	6	4	1	1
22q11.21	16,15	21,17	6	4	3	0	1	
LOSS	6q16-q25	100	154	75	4	3	1	0
	8p23-p22	4	15	14	3	3	0	0
	11q24-q25	128	133	8	4	3	0	1
	17p13.3	0,34	0,96	6	4	3	1	0

Table 6. Selection of pathways differentially expressed in NKTCL tissues compared to normal NK cells or PTCL, NOS*.

Pathway name	Median <i>P</i>-value (compared to normal NK cells)	Median <i>P</i>-value (compared to PTCL, NOS)
Apoptosis		
Apoptosis	0.002	< 0.002
Regulation of BAD phosphorylation	0.109	< 0.018
PTEN dependent cell cycle arrest and apoptosis	0.246	< 0.015
FAS signalling pathway	0.257	< 0.006
Cytotoxicity		
Natural killer cell mediated cytotoxicity	0.002	< 0.0001
Ras-Independent pathway in NK cell-mediated cytotoxicity	0.325	< 0.0001
Cell adhesion molecules / extracellular matrix receptor interaction		
Cell communication	0.001	< 0.016
ECM receptor interaction	0.001	< 0.016
Focal adhesion	0.001	< 0.023
Cell adhesion molecules	0.002	< 0.012
Leukocyte transendothelial migration	0.002	0.371
Inhibition of matrix metalloproteinases	0.003	0.018
Integrin signalling pathway	0.003	0.484
Cell cycle		
Regulation of p27 during phosphorylation	< 0.006	0.008
Cyclin E destruction pathway	< 0.041	0.003
Chemokines / cytokines		
Cytokine cytokine receptor interaction	0.002	< 0.001
Signal transduction		
JAK-STAT signaling pathway	0.002	0.01
MAPK signaling pathway	0.002	0.015
mTOR signaling pathway	0.002	0.06
NF-κB signaling pathway	0.002	0.06
TGFβ signaling pathway	0.002	0.019
VEGF signaling pathway	0.002	0.418
Notch signaling pathway	< 0.005	0.025
Wnt signaling pathway	< 0.005	< 0.013
AKT signalling pathway	0.14	< 0.001

*: with a median *P*-value < 0.02 compared to either normal NK cells or PTCL, NOS.

FIGURE LEGENDS.

Figure 1. Validation of gene expression profiling by immunohistochemistry.

Representative NKTCLs disclosed cytoplasmic staining of neoplastic cells for (A) gzm H, (B) EBI3, (C) VEGFA, nuclear localization of (D) pSTAT3, (E) pAKT, cytoplasmic and nuclear staining of (F) RelA, and positivity for (G) PDGFR α and (H) pPDGFR α . Images were captured with a Zeiss Axioskop2 microscope (Zeiss, Oberkochen, Germany). Photographs were taken with a DP70 Olympus camera (Olympus, Tokyo, Japan). Image acquisition was performed with Olympus DP Controller 2002, and images were processed with Adobe Photoshop v7.0 (Adobe Systems, San Jose, CA). Original magnifications: x400 (A-H).

Figure 2. Unsupervised clustering of seven NKTCLs, two NKTCL-derived cell lines and 16 PTCLs, NOS. Dendrogram of 23 lymphoma tissues and two cell lines based on principal component analysis demonstrated two major clusters of NKTCL including tumor-derived cell lines and PTCL, NOS, respectively. T1-7: seven NKTCL samples, SNK6, SNT8, C1-16: 16 PTCL, NOS samples.

Figure 3. Genomic profiles of NKTCL. Pangenomic view of eight NKTCL tissue samples. The horizontal axis represents the genomic order, and the vertical axis represents the number of samples with gains or losses. Gains are represented as red bars and losses are represented as green bars.

Figure 4. Quantification of selected genes by qRT-PCR analysis. qRT-PCR analysis for (A) *MET*, (B) *TNFRSF21*, (C) *CCND3*, (D) *CCL2*, and (E) *PRDMI*, *ATG5*, *AIM1*, and *HACE1* in NKTCL primary tumors and cell lines. The results are expressed as relative fold change compared to resting CD3⁻/CD56⁺ NK cells sorted from peripheral blood. Quantifications were done in duplicate and mean values and standard deviation were calculated for each transcript. (A-D) In agreement with the microarray results, mRNA levels of *MET*, *CCL2*, *TNFRSF21* are increased in NKTCL primary tumors compared to normal NK

cells whereas *CCND3* mRNA is reduced (E) The analysis of four putative tumor suppressors in 6q21 region show that the transcripts levels of *HACE1*, *AIM1* and *ATG5* are reduced in primary tumors and cell lines whereas the mRNA level of *PRDMI* is increased in primary tumors, due to a wide variation from case to case (not shown).

Figure 5. Cellular programs deregulated in NKTCL. Representative molecular pathways differentially expressed in NKTCLs by comparison to either normal NK cells (A. JAK-STAT, B. angiogenesis, E. apoptosis), [normal B cells and ABC-DLBCL \(C. NF- \$\kappa\$ B\), normal NK cells and normal B cells \(D. AKT\)](#), or PTCL, NOS (F. cytotoxicity) were illustrated. For each line, green corresponds to the minimal intensity value (min), red corresponds to the maximal intensity value (max), and black corresponds to $(\text{min} + \text{max})/2$. Several genes related to JAK-STAT, angiogenesis, and apoptosis-related pathways are overexpressed in NKTCLs compared to normal NK cells, and genes related to the cytotoxicity-related pathway are also overexpressed in NKTCLs compared to PTCL, NOS. [Many genes in the NF- \$\kappa\$ B and AKT signaling pathways are overexpressed in NKTCLs compared to normal B cells, with a molecular signature similar to that of ABC-DLBCL in NK- \$\kappa\$ B pathway.](#) The expression data of *PDGFRA* in NKTCLs, 2 NKTCL-derived cell lines, and normal NK cells is highlighted. T1-7: seven NKTCL samples, C1-16: 16 PTCL, NOS samples, AcNK, AcNK02, AcNK08, AcNK24: activated NK cells, ReNK, ReNK.: resting NK cells, [CB.1-8 and CB.11: nine centroblasts samples, CC.1-8 and CC.11: nine centrocytes samples, ABC.2024-2195: 15 ABC-DLBCL samples.](#)

Figure 6. Proliferation of NKTCL-derived cell lines in the presence of imatinib mesylate. SNK6, MEC04, and U937 cells were incubated for 72 hours in media with or without imatinib mesylate at concentrations of 1, 3, and 6 μ M. Imatinib induced concentration-dependent growth inhibition of MEC04 cells. The effect on SNK6 was not significantly different from that observed on the myelomonocytic U937 cell line. The horizontal axis is the

concentration of imatinib mesylate. The vertical axis is the percentage of control proliferation. Bars indicate the SEM of triplicate experiments.

Figure 7. Hypothetical representation of signaling pathways involved in NKTCL. The interactions of PDGF, AKT, and JAK-STAT signaling pathways may contribute to the angiogenesis, immunosuppression, proliferation and survival of NKTCL.

Figure 1.

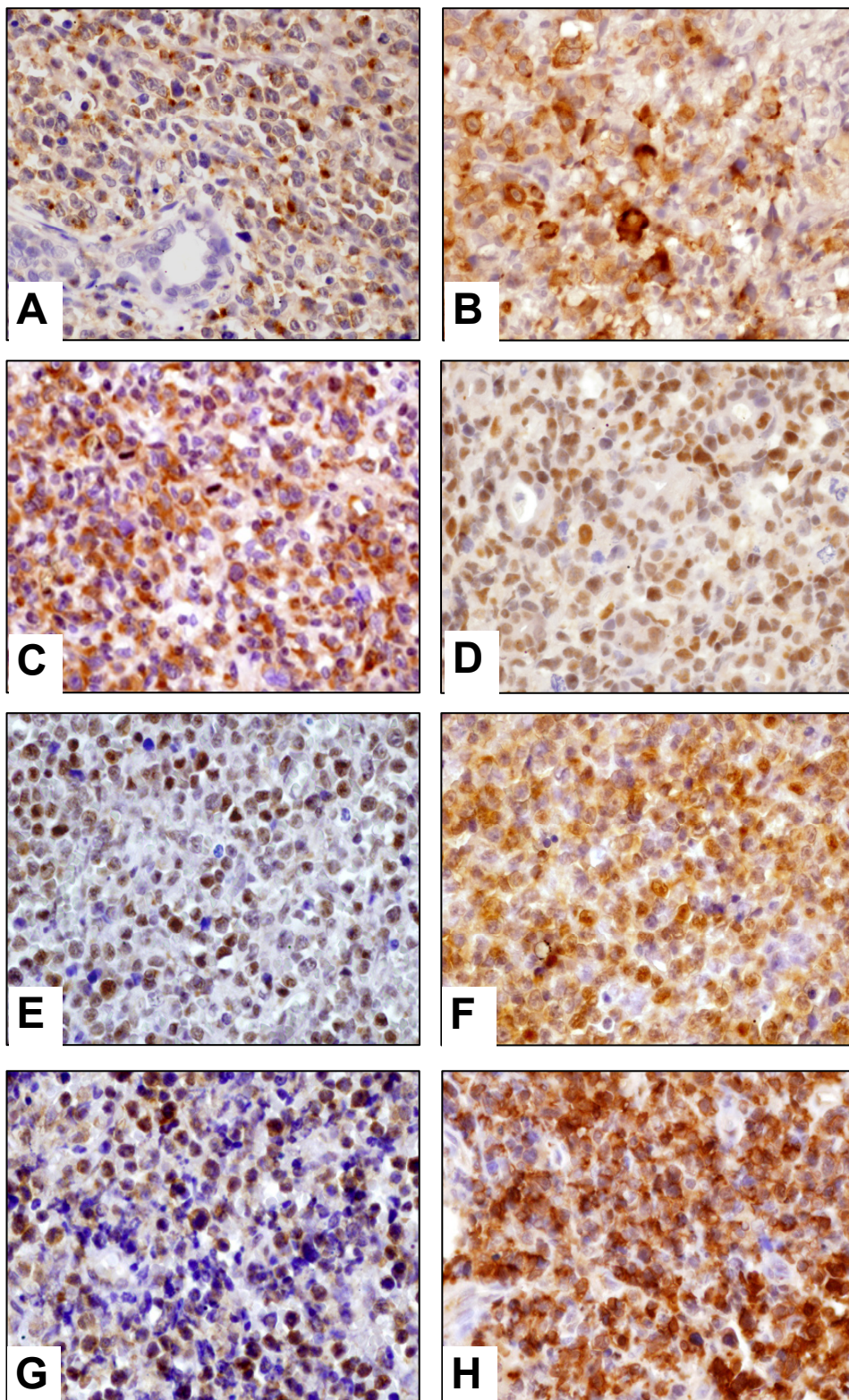


Figure 2.

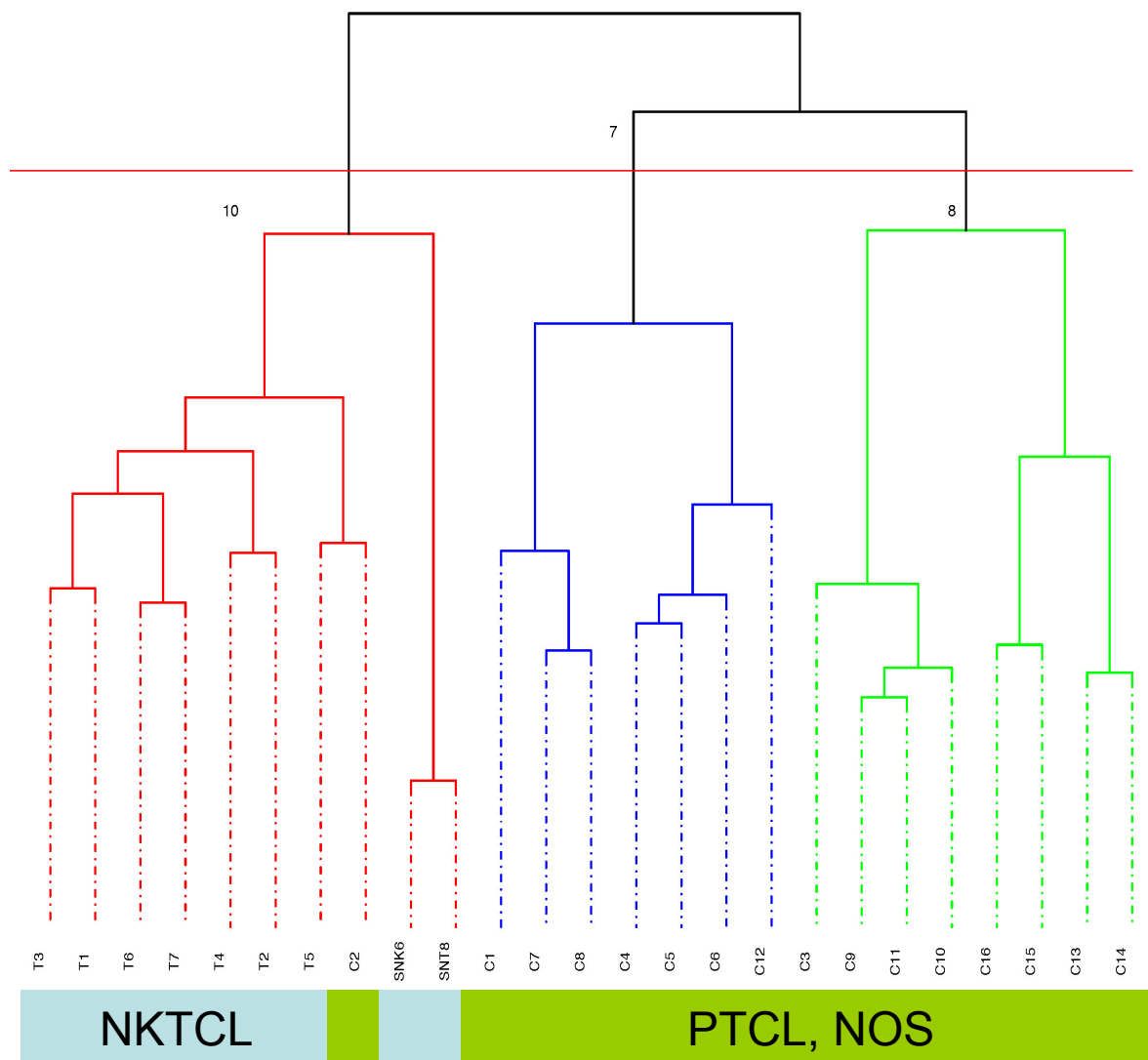


Figure 3.

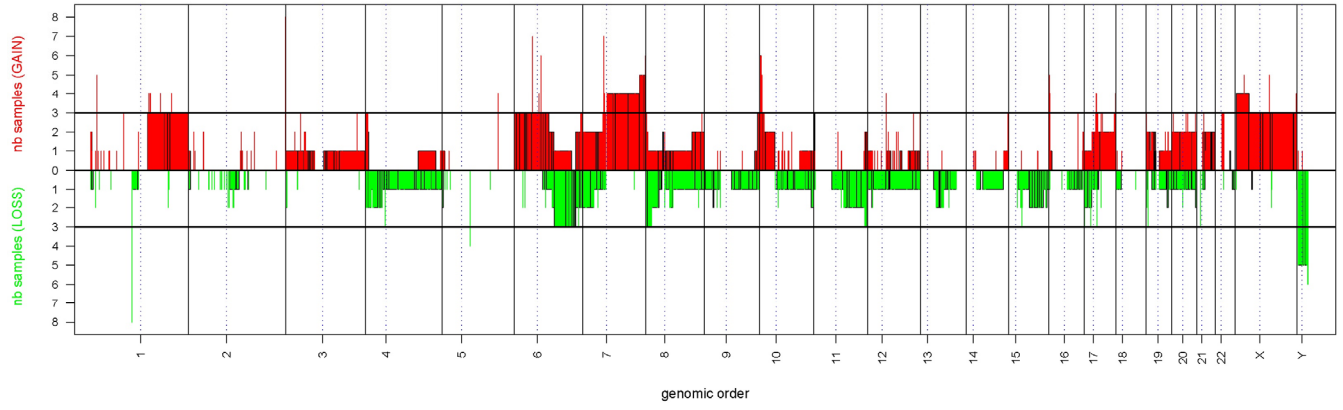


Figure 4.

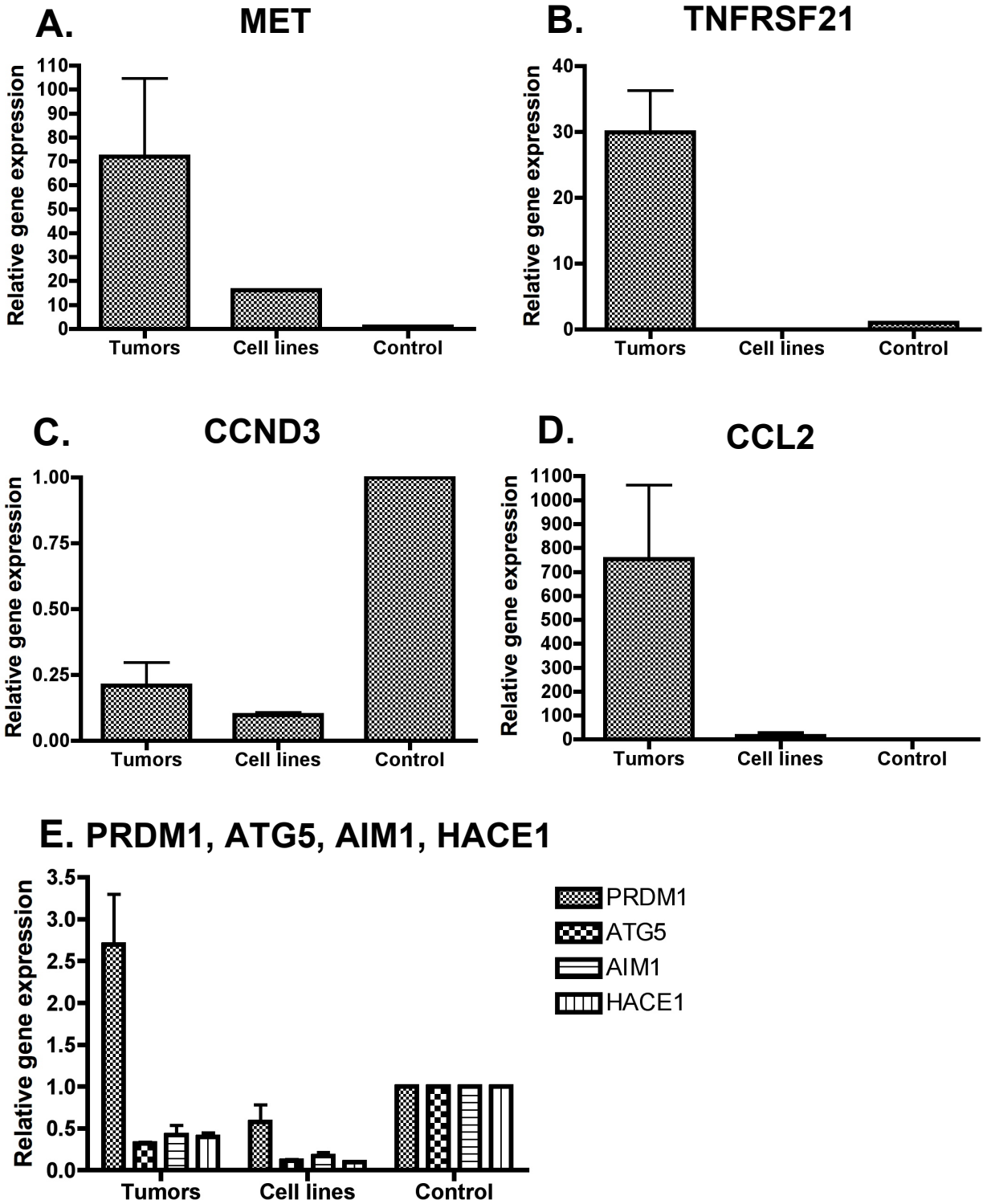


Figure 6.

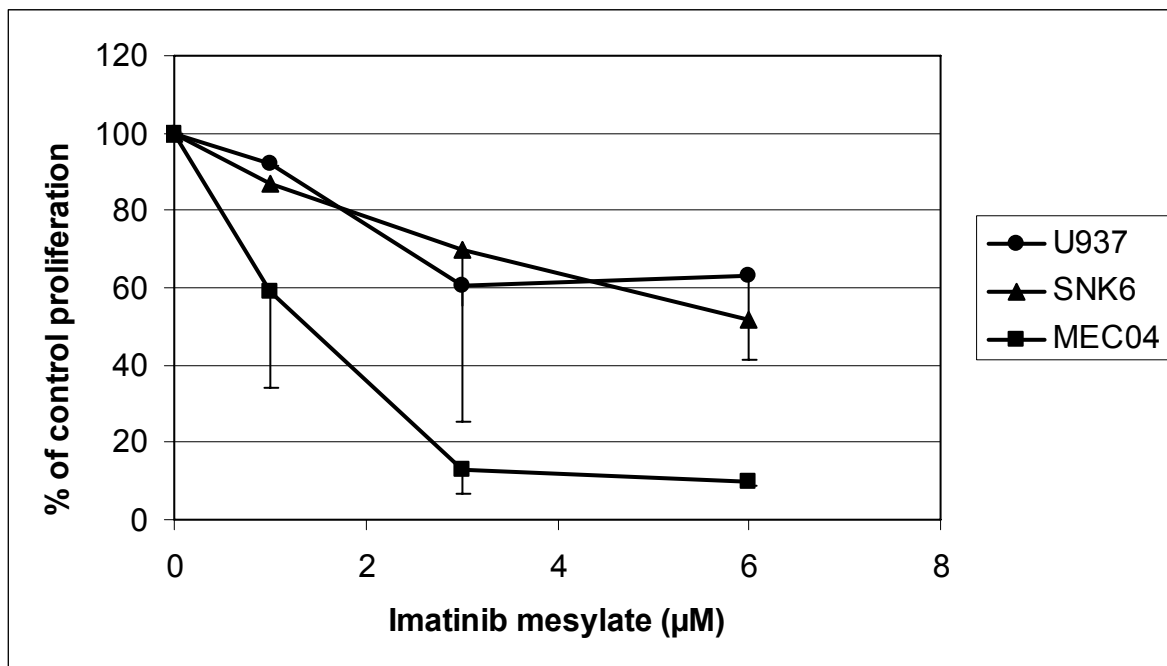


Figure 7.

